Nitrous oxide reduction by two partial denitrifying bacteria requires denitrification intermediates that cannot be respired

Breah LaSarre[1,a], Ryan Morlen[2], Gina C. Neumann[1,b],
Caroline S. Harwood[2], and James B. McKinlay[1]*

[1] Department of Biology, Indiana University, Bloomington, IN
[2] Department of Microbiology, University of Washington, Seattle, WA

*Corresponding author: jmckinla@iu.edu

Current address:
[a] Department of Plant Pathology, Entomology, and Microbiology, Iowa State University, Ames, Iowa, USA
[b] Benson Hill, St. Louis MO, USA

Abstract

Denitrification is a form of anaerobic respiration wherein nitrate (NO_3^-) is sequentially reduced via nitrite (NO_2^-), nitric oxide, and nitrous oxide (N_2O) to dinitrogen gas (N_2) by four reductase enzymes. Partial denitrifying bacteria possess only one, or some, of these four reductases and use them as independent respiratory modules. However, it is unclear if partial denitrifiers sense and respond to denitrification intermediates outside of their reductase repertoire. Here we tested the denitrifying capabilities of two purple nonsulfur bacteria, *Rhodopseudomonas palustris* CGA0092 and *Rhodobacter capsulatus* SB1003. Each had denitrifying capabilities that matched their genome annotation; CGA0092 reduced NO_2^- to N_2 and SB1003 reduced N_2O to N_2. For each bacterium, N_2O reduction could be used for both electron balance during growth on electron-rich organic compounds in light and for energy transformation via respiration in the dark. However, N_2O reduction required supplementation with a denitrification intermediate, including those for which there was no associated denitrification enzyme. For CGA0092, NO_3^- served as a stable, non-catalyzable molecule that was sufficient to activate N_2O reduction. Using a β-galactosidase reporter we found that NO_3^- acted, at least in part, by stimulating N_2O reductase gene expression. In SB1003, NO_2^-, but not NO_3^-, activated N_2O reduction but NO_2^- was slowly removed, likely by a promiscuous enzyme activity. Our findings reveal that partial denitrifiers can still be subject to regulation by denitrification intermediates that they cannot use.

Importance. Denitrification is a form of microbial respiration wherein nitrate is converted via several nitrogen oxide intermediates into harmless dinitrogen gas. Partial denitrifying bacteria, which individually have some but not all denitrifying enzymes, can achieve complete denitrification as a community by cross-feeding nitrogen oxide intermediates. However, the last intermediate, nitrous oxide (N_2O), is a potent greenhouse gas that often escapes, motivating efforts to understand and improve the efficiency of denitrification. Here we found that at least some partial denitrifying N_2O reducers can sense and respond to nitrogen oxide intermediates that they cannot otherwise use. The regulatory effects of nitrogen oxides on partial denitrifiers are thus an important consideration in understanding and applying denitrifying bacterial communities to combat greenhouse gas emissions.

Introduction

Denitrification is a multistep respiratory pathway that sequentially reduces nitrate (NO_3^-) via nitrite (NO_2^-), nitric oxide (NO), and nitrous oxide (N_2O) to dinitrogen gas (N_2) (1, 2) (Fig. 1A). Denitrifying bacteria are important in several contexts. Denitrifiers in the human gut help fight pathogens and maintain vascular homeostasis through the generation of NO_2^- and NO (3). Denitrification is also important to the global nitrogen cycle, returning nitrogen to the atmosphere as N_2. However, N_2O often escapes denitrifying communities before it can be reduced to N_2. N_2O is a potent greenhouse gas that damages the ozone layer (4). N_2O emissions have increased to concerning levels, primarily due to transformation of NO_3^- in agricultural fertilizers to N_2O by naturally occurring denitrifying bacteria in the soil (5, 6). Thus, there is a need to better understand and improve the efficiency of denitrification.

Many bacteria lack a complete denitrification pathway and are thus called partial or truncated denitrifiers (7-11). Partial denitrifiers use single or multiple steps of the pathway as independent respiratory modules (1, 2). Although incapable of reducing NO_3^- to N_2 on their own, partial denitrifiers are important contributors to complete denitrification as a community process, with intermediates cross-fed between community members that have different segments of the pathway (7-12). Notably, nitrogen oxides (NO_3^-, NO_2^-, NO, or N_2O) not only serve as substrates for denitrification reductases can also act as regulators of denitrification. Although regulatory roles have been well-characterized in bacteria capable of complete denitrification, regulatory roles in partial denitrifiers have received comparatively less attention. In particular, it is unclear if the regulatory effects of nitrogen oxides in partial denitrifiers matches their reductase repertoire.

Here we characterized the ability of two purple non-sulfur bacteria (PNSB) that are putative partial denitrifiers, *Rhodopseudomonas palustris* CGA0092 and *Rhodobacter capsulatus* SB1003, to carry out denitrification under photoheterotrophic and chemoheterotrophic conditions. Under phototrophic conditions, where light is the energy source, we tested if nitrogen oxides can serve as an essential electron acceptor to maintain electron balance during growth on the electron-rich substrate butyrate. Under chemotrophic conditions, we tested if nitrogen oxides can serve as an essential electron acceptor to generate energy via oxidative phosphorylation. As expected, each bacterium was only able to grow using the nitrogen oxides for which corresponding reductases were annotated in their genomes. However, N_2O utilization required supplementation with additional nitrogen oxides other than N_2O, including nitrogen oxides for which there was no predicted reductase and which did not support growth on their own. Our results indicate that at least some partial denitrifiers require nitrogen oxides that they cannot respire to reduce N_2O.

Results

***R. palustris* CGA0092 has a partial denitrification pathway.** *R. palustris* is one of the most metabolically versatile PNSB (13), yet little is known about its ability to respire anaerobically. Unlike some other model PNSB, CGA009, and its derivative CGA0092 (14) used herein, cannot grow via respiration with dimethylsulfoxide (15-17). However, according to its genome sequence, it should be capable of partial denitrification, as it has putative enzymes for converting

NO_2^- to N_2 (10, 13) (Fig. 1B). Expanding on past analyses by others (10, 13), we used PSI-BLAST to verify that there are no genes with significant similarity to *nar, nap,* or *nas* nitrate reductase genes nor to *nasB*, *nirB, nirD, nirA*, *nrf*, or eight-heme nitrite reductase genes (Table S1) (18).

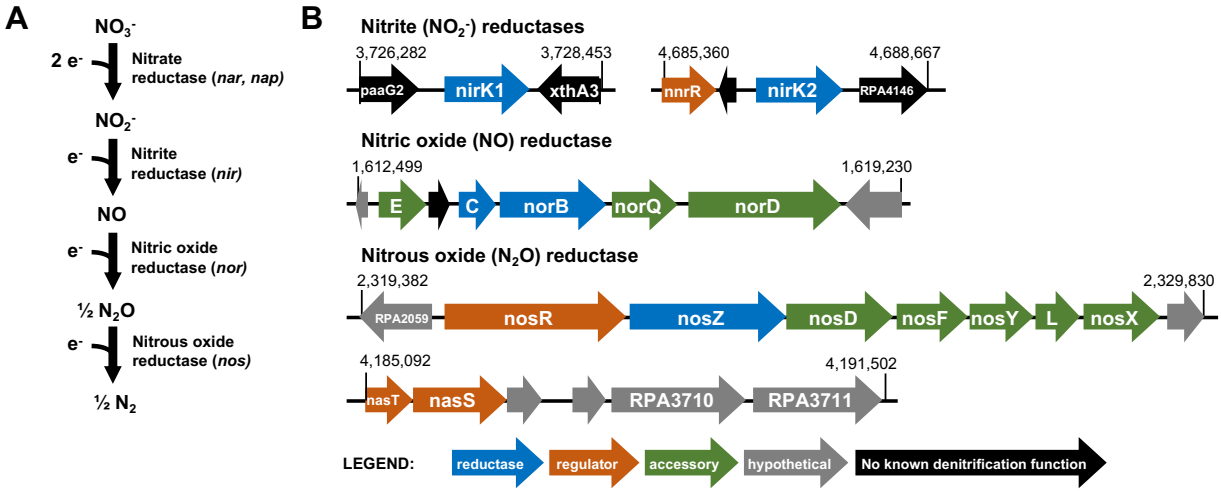

Fig. 1. General denitrification pathway (A) and denitrification genes annotated in *R. palustris* CGA0092 (B). Numbers indicate the chromosome nucleotide positions. Several CRP/Fnr-family transcriptional regulators with >25% sequence identity to known denitrification regulators are not shown.

When incubated anaerobically in darkness, PNSB typically use electron acceptors to establish a proton motive force and generate ATP. When incubated in light, PNSB generate ATP by photophosphorylation but electron acceptors, such as CO_2 or $NaHCO_3$, are required for growth on electron-rich compounds like butyrate to prevent an accumulation of reduced electron carriers that halts metabolism; butyrate contains more electrons than can be incorporated into biomass and so the excess electrons must be deposited on an electron acceptor or released as H_2 (19, 20). Given that *R. palustris* grows best in light, we first examined if it could use denitrification intermediates as electron acceptors during growth with butyrate.

In agreement with the apparent lack of NO_3^- reductase in the CGA0092 genome (Fig. 1B), phototrophic growth on butyrate was not supported when supplemented with a wide range of $NaNO_3$ concentrations (Fig. 2A). However, growth was observed when CGA0092 was provided with 1mM $NaNO_2$ (Fig. 2A). We determined that this concentration was near the toxicity limit because it caused a lag in phototrophic growth on succinate, which does not require supplementation with an electron acceptor (Fig. 2B). We verified NO_2^- utilization using the colorimetric Griess assay. All of the NO_2^- removed could be accounted for in the accumulated N_2 and N_2O, as measured by gas chromatography (Fig. 2C). N_2 and N_2O levels were, in fact, higher than what could be explained by conversion of the supplied NO_2^-, although not significantly different from the expected 1:1 correspondence. If real, the excess nitrogen was likely due to contamination with atmospheric N_2 during sampling and an inability to distinguish N_2O from CO_2 produced by other metabolic reactions (CO_2 and N_2O coeluted in our gas chromatography method).

Generation of N_2 from NO_2^- indicated that the latter three reductases for denitrification are active in CGA0092. We did not directly address reduction of exogenously added NO because it is highly toxic and would likely be impossible to add in amounts that would be practical to yield observable growth. We directly addressed N_2O reduction by providing CGA0092 with a headspace of 100% N_2O. However, no growth was observed within 15 days (Fig. 2A), suggesting that N_2O alone cannot activate N_2O reduction.

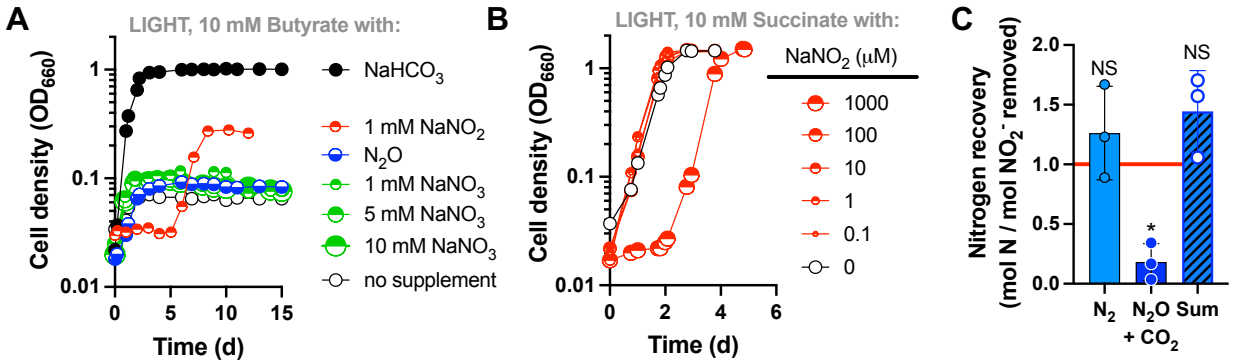

Fig. 2. $NaNO_2$ supports phototrophic growth of CGA0092 on butyrate within toxicity limits. A. Phototrophic growth with butyrate and various potential electron acceptors. Single representatives are shown. Similar trends were observed for three biological replicates except for conditions exploring different $NaNO_3$ concentrations where only single representatives were used. **B.** Phototrophic growth with succinate, a condition that readily supports growth without supplementation with an electron acceptor, with various concentrations of $NaNO_2$ to identify the toxicity limit. Cultures had a 100% Ar headspace unless N_2O is indicated (100% N_2O). **C.** Proportion of NO_2^- recovered as N_2 and N_2O. All of the supplied NO_2^- was removed. N_2O peak area includes a minor contribution of CO_2 due to coelution during gas chromatography. Each point represents an independent biological replicate. *, significantly different from 1 ($p < 0.05$); NS, not significantly different from 1.0 ($p > 0.05$), determined by a one sample t and Wilcoxon test.

Photoheterotrophic N_2O reduction by CGA0092 requires $NaNO_2$ or $NaNO_3$. In some bacteria, denitrification intermediates other than N_2O enhance, or are required for, N_2O reduction (1, 2, 21-23). For example, NO_2^- induces N_2O reductase at the transcriptional level via the regulatory protein NnrR, though NO_2^- might first need to be converted to NO (23). NO_3^- induces N_2O reductase via NasTS regulatory proteins and an anti-terminator mechanism that affects transcription of *nos* genes (24, 25). CGA0092 encodes NnrR upstream of NirK2 and NasTS homologs upstream of a gene cluster encoding a potential nitrite/sulfite reductase (RPA3710-11; Fig. 1B). We thus tested if $NaNO_2$ or $NaNO_3$ could enable growth with N_2O. In agreement with our hypothesis, micromolar amounts of $NaNO_2$ as low as 1 μM stimulated growth with N_2O, with final cell densities increasing in accordance with the amount of $NaNO_2$ added (Fig. 3A). $NaNO_2$ at 100 μM caused a 4-day lag in growth (Fig. 3A), suggesting that this level of NO_2^- was slightly toxic under these conditions. Notably, the increase in final cell density afforded by high amounts of $NaNO_2$ depended on the presence of N_2O, as growth with 100 μM $NaNO_2$ alone was much lower (Fig. 3A). This indicated that N_2O was being used as the primary electron acceptor in the presence of NO_2^-, despite that N_2O could not serve as an electron acceptor when provided alone (Fig. 2A). We speculate that exhaustion of NO_2^- eliminated the activation of N_2O

reduction, thereby eliminating the ability to use N_2O as an electron acceptor; consequently, growth on butyrate with N_2O lasts only as long as the pool of $NaNO_2$.

Despite lacking NO_3^- reductase, $NaNO_3$ was also sufficient to stimulate phototrophic growth on butyrate with N_2O (Fig. 3B). Similar growth trends were observed between 1 µM to 10 mM $NaNO_3$, indicating that $NaNO_3$ is relatively non-toxic and suggesting that NO_3^- was not being reduced. Indeed, NO_3^- levels were stable when we used 0.1 mM $NaNO_3$ to stimulate photoheterotrophic N_2O reduction (Fig. 3C). The amount of N_2O provided, all of which was ultimately removed, was linearly correlated with N_2 generated (Fig. 3C), although we again observed more N_2 generated than should be possible from the N_2O provided, likely due to contamination with atmospheric N_2. Culture growth and butyrate consumed were also linearly correlated with N_2O supplied (and removed), further demonstrating the use of N_2O as an electron acceptor (e.g., in place of $NaHCO_3$; Fig. 2A) for phototrophic growth with butyrate.

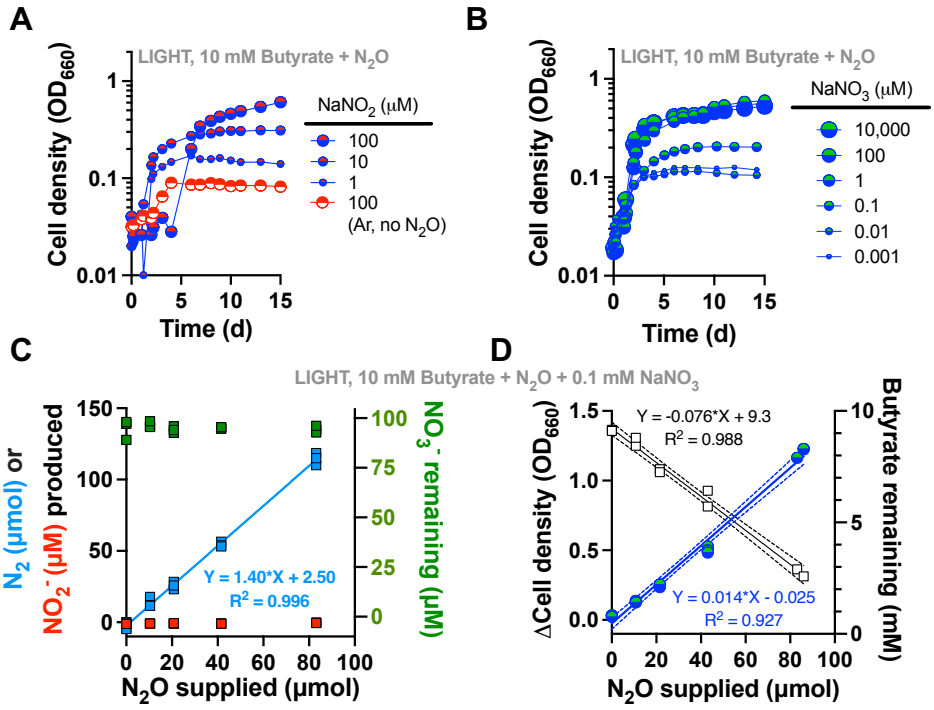

Fig. 3. $NaNO_2$ or $NaNO_3$ is required for phototrophic N_2O utilization by CGA0092. A. Phototrophic growth with butyrate +/- N_2O and different concentrations of $NaNO_2$. The 'Ar, no N_2O' control had a 100% argon headspace. **B.** Phototrophic growth with butyrate + N_2O and different concentrations of $NaNO_3$. Single representatives were surveyed. **C, D.** Changes in N_2, NO_3^-, NO_2^-, cell density, and butyrate in N_2O-limited cultures. Measurements were taken at inoculation and when the maximum cell density was reached. Each point represents a single independent culture. All N_2O was removed by stationary phase. Linear regression for NO_3^- (**C**) gave a slope that was not significantly different from zero ($p = 0.57$).

To determine if the requirement of $NaNO_3$ or $NaNO_2$ for N_2O reduction is manifested at the level of N_2O reductase expression (the combination of transcription and translation), we created a reporter that fused the region upstream of *nosR*, which should contain both a transcriptional promoter and a ribosomal binding site, to the *lacZ* gene at the start codon and integrated the

reporter into the CGA0092 chromosome. We then grew the resulting reporter strain (CGA4070) under phototrophic conditions with acetate, a condition where an electron acceptor supplement is not required, and added either NaCl (negative control), $NaNO_3$, $NaNO_2$, or N_2O as possible inducers of expression. In agreement with growth trends (Fig. 3), $NaNO_3$ and $NaNO_2$, but not N_2O, led to a significant, albeit low (1.6 – 2.4-fold), increase in LacZ activity over the NaCl control (Fig. 4). Thus, $NaNO_3$ and $NaNO_2$ are inducers of *nos* gene expression, although the relatively small effect suggests that there might be additional levels of regulatory control.

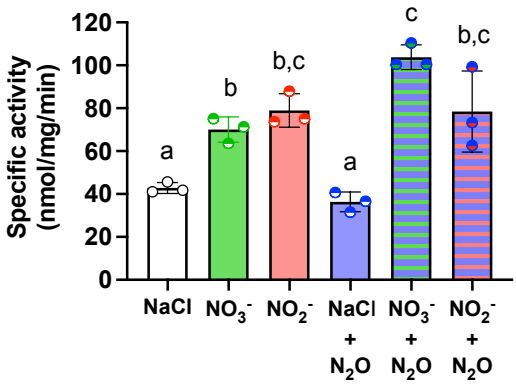

Fig. 4. $NaNO_3$ and $NaNO_2$, but not N_2O, positively affect *nosR* expression. β-galactosidase measurements were made in cell extracts of CGA4070, which harbors a chromosomally integrated *nosR* promoter–*lacZ* fusion. CGA4070 was grown phototrophically with 23 mM acetate and 0.1 mM NaCl, $NaNO_3$ or $NaNO_2$. Cultures received 4 ml N_2O, where indicated. Each point represents a single independent culture. All values were corrected for a background *o*-nitrophenol production rate of 8.7 nmol/mg/min as measured in cell extracts from CGA0092 grown under identical conditions with 0.1 mM NaCl or $NaNO_3$; activity was not significantly different between conditions with NaCl or $NaNO_3$. Floating letters indicate significant differences between strains (One-way ANOVA with Tukey post-test)$p < 0.5$).

N_2O plus $NaNO_3$ can rescue photoheterotrophic growth of *R. palustris* Calvin cycle mutants. Under most photoheterotrophic growth conditions, the CO_2-fixing Calvin cycle is essential to maintain electron balance, even on relatively oxidized substrates like succinate (19, 26, 27). To distinguish this essential electron balancing role from the Calvin cycle's better known role in carbon assimilation, alternative electron acceptors are a useful tool because they permit growth of Calvin cycle mutants (28, 29). Thus far, the only method known to allow growth of *R. palustris* Calvin cycle mutants under conditions where the cycle is normally essential was via NifA* mutations that result in constitutive nitrogenase activity (19, 26, 27). NifA* mutants dispose of excess electrons as H_2, an obligate product of the nitrogenase reaction. However, our results suggested that N_2O could be used as an electron acceptor to grow *R. palustris* Calvin cycle mutants without additional genetic intervention. Indeed, N_2O with $NaNO_3$ rescued an *R. palustris* Calvin cycle mutant (ΔCalvin) during phototrophic growth on succinate (Fig. 5). N_2O reduction resulted in more immediate growth than a NifA* mutation. However, growth eventually slowed and the culture reached a lower final cell density that the ΔCalvin NifA* mutant (Fig. 5). Gas chromatographic analysis of headspace samples confirmed that growth of cultures with N_2O plus $NaNO_3$ was not due to spontaneous mutations that enabled H_2 production (i.e., no H_2 was detected; data not shown).

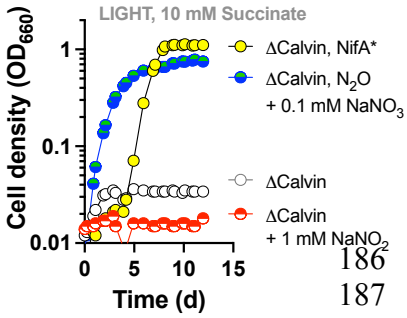

Fig. 5. N_2O plus $NaNO_3$ supports phototrophic growth of an *R. palustris* Calvin cycle deletion mutant. Cultures had a 100% Ar headspace unless N_2O is indicated (100% N_2O). Single representatives are shown. Similar trends were observed for three biological replicates. ΔCalvin is strain CGA4008; ΔCalvin, NifA* is strain CGA4011.

$NaNO_3$ does not improve *R. palustris* photoheterotrophic growth with $NaNO_2$. We wondered if $NaNO_3$ might also improve growth with NO_2^-, perhaps by stimulating NO_2^- reductase activity. However, supplementation with $NaNO_3$ did not affect photoheterotrophic growth trends on butyrate with 1 mM $NaNO_2$, even when $NaNO_3$ was also added to starter cultures as a possible 'pre-inducing' condition (Fig. 6A). The same strategy also did not decrease the lag phase during phototrophic growth on succinate with 1 mM $NaNO_2$ (Fig. 6B).

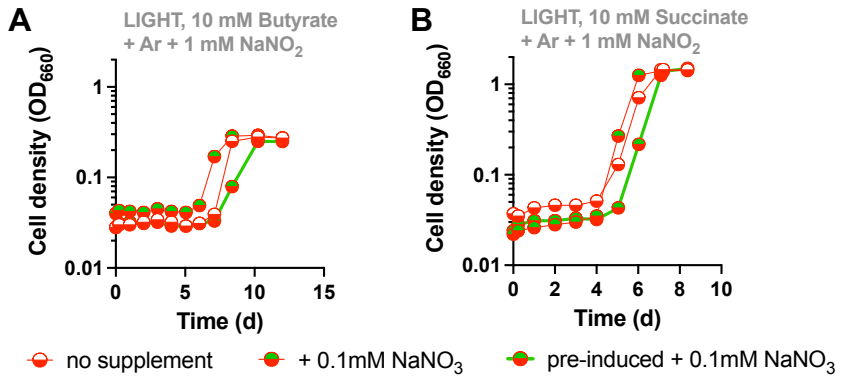

Fig. 6. $NaNO_3$ does not improve growth trends when $NaNO_2$ is present as an essential electron sink (A) or as a toxic compound (B). Single representatives are shown. Similar trends were observed for three biological replicates.

$NaNO_3$ is required for anaerobic respiration with N_2O by CGA0092 in the dark. Without access to light, many PNSB can grow chemoheterotrophically via anaerobic respiration. We tested if $NaNO_2$ or N_2O could support chemoheterotrophic growth by CGA0092 in the dark. Acetate and butyrate were chosen as two carbon sources that are metabolized via similar pathways but contain different amounts of electrons (19). Unlike phototrophic conditions (Fig. 2), supplementation with either 0.3 or 1 mM $NaNO_2$ did not support observable growth in the dark with either acetate or butyrate within 15 days. In contrast, N_2O supported growth with either acetate or butyrate but only when $NaNO_3$ was also provided (Fig. 7). Because growth was slower with acetate than with butyrate (doubling time ± SD = 88 ± 2 h vs 51 ± 3, respectively), we performed further analyses with butyrate. As during phototrophy (Fig. 3), chemotrophic N_2 production, culture growth, and butyrate consumption were linearly correlated with the amount of N_2O provided (Fig. 7C, D). All or nearly all N_2O was removed while NO_3^- levels remained stable, without NO_2^- production (Fig. 7C).

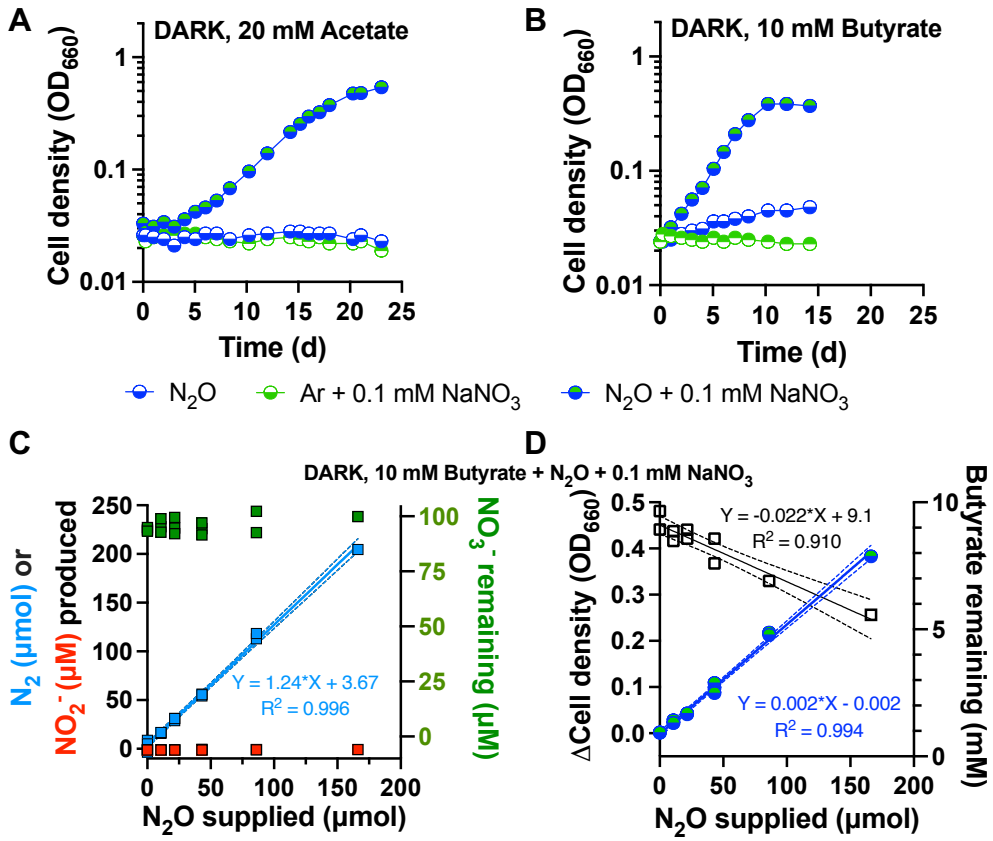

Fig. 7. $NaNO_3$ is required for N_2O respiration by CGA0092 in the dark with acetate (A) or butyrate (B). Single representatives are shown. Similar trends were observed for three biological replicates. Cultures had a 100% Ar headspace or 100% N_2O headspace as indicated. **C, D.** Changes in N_2, NO_3^-, cell density, and butyrate in N_2O-limited cultures. Measurements were taken at inoculation and when the maximum cell density was reached. Each point represents a single independent culture. Most or all N_2O was removed by stationary phase. Linear regression for NO_3^- (**C**) gave a slope that was not significantly different from zero ($p = 0.11$).

The chemotrophic growth rate and growth yield with butyrate was 24% and 17%, respectively, of those observed under phototropic N_2O-reducing conditions (Table 1). However, the specific rate of N_2O reduction was 1.4-fold higher under chemotrophic conditions (Table 1), suggesting that the rate of N_2O reduction needed to support electron balance under phototrophic conditions is less than that possible when N_2O reduction is needed for energy transformation. In agreement with the lower growth yield, the N_2O product yield was 3.3-fold higher under chemotrophic conditions (Table 1), indicating that more electrons from butyrate were directed to energy transformation compared to biosynthesis during chemotrophic growth.

$NaNO_2$ is required for phototrophic N_2O reduction by *R. capsulatus* SB1003. We wondered if the requirement for non-catalyzable denitrification intermediates for N_2O utilization was specific to *R. palustris* or was also true in other partial denitrifiers. To examine this possibility, we turned to *R. capsulatus* SB1003, which stood out as an easily cultivatable and phylogenetically distant PNSB that is annotated to only have N_2O reductase (10) (Fig. 8A).

Using PSI-BLAST, we built upon past analyses (10) and confirmed that SB1003 does not have genes with significant similarity to known assimilatory and dissimilatory NO_3 and NO_2 reductase genes (Table S1). As predicted, phototrophic growth of SB1003 on butyrate was not supported by $NaNO_3$ or $NaNO_2$ (Fig. 8B), although our ability to assess the latter was limited by the sensitivity of SB1003 to $NaNO_2$ concentrations > 0.5 mM (Fig. 8C). Similar to what was observed for *R. palustris*, N_2O alone did not support phototrophic growth of SB1003 (Fig. 8B). However, supplementation with 0.1 mM $NaNO_2$, but not $NaNO_3$, led to phototrophic growth on butyrate with N_2O (Fig. 8B). Also, N_2 production, growth, and butyrate production were linearly correlated with the amount of N_2O provided (Fig. 8D, E), with all or nearly all N_2O removed. However, unlike with *R. palustris*, levels of the stimulating compound, in this case NO_2^-, were not stable. NO_2^- concentration declined with a roughly linear correlation to the amount of N_2O provided (Fig. 8D). NO_3^- concentrations remained close to zero (Fig. 8D), suggesting that NO_2^- was reduced, rather than oxidized. The specific rate of N_2O reduction was 300-times higher than that of NO_2^- reduction (Table 1). This disparity suggests that NO_2^- removal was likely due to a promiscuous enzyme activity or a growth-correlated abiotic factor rather than due to an unannotated bonafide NO_2^- reductase.

Table 1. Growth and metabolic parameters from N_2O-reducing conditions with butyrate.

Strain, growth condition	Sp. growth rate (d^{-1})	Doubling time (d)	Sp. N_2O reduction rate (fmol/CFU/d)	Sp. NO_2^- reduction rate (fmol/CFU/d)	Growth yield (CFU/pmol N_2O)	Growth yield (CFU/pmol butyrate)	N_2O product yield (mol/mol butyrate)
CGA0092, light	1.36 ± 0.09	0.51 ± 0.04	1877 ± 182	ND	70 ± 5	90 ± 10	1.3 ± 0.1
CGA0092, dark	0.32± 0.02	2.20 ± 0.16	2645 ± 221	ND	12 ± 0	50 ± 10	4.3 ± 0.8
SB1003, light	1.32 ± 0.18	0.53 ± 0.07	1503 ± 229	5 ± 3	87 ± 6	105 ± 5	1.6 ± 0.3
SB1003, dark	0.79 ± 0.16	0.87 ± 0.02	6332 ± 1348	5 ± 4	13 ± 0	75 ± 10	5.9 ± 0.8

Values show averages ± 95% CI. Doubling time = ln2/growth rate. Specific (Sp) reduction rates were determined by multiplying the growth rate by the slope of a linear regression of product vs cell density (30, 31) from N_2O-limited cultures. Colony forming units (CFU) were obtained using a conversion factor of 1 OD_{660} = 5 x 10^8 CFU/ml (32). Product yields were determined by linear regression using measurements of N_2O, NO_2^-, and butyrate from N_2O-limited cultures.

$NaNO_2$ is required for anaerobic respiration with N_2O by SB1003 in the dark. SB1003 could also respire N_2O in the dark with butyrate, but again only when $NaNO_2$ was also present (Fig. 9A). Most or all N_2O was converted to N_2 when limiting amounts of N_2O was provided in the presence of 0.1 mM $NaNO_2$ (Fig. 9B). N_2O supplied also showed linear correlation with culture growth and butyrate consumption (Fig. 9C). Although only a small amount, some NO_2^- was likely removed during N_2O reduction because the linear correlation of NO_2^- levels with N_2O supplied was negative and significantly different from zero (Fig. 9B). The specific NO_2^- reduction rate was 3-orders of magnitude slower than the specific N_2O reduction rate (Table 1),

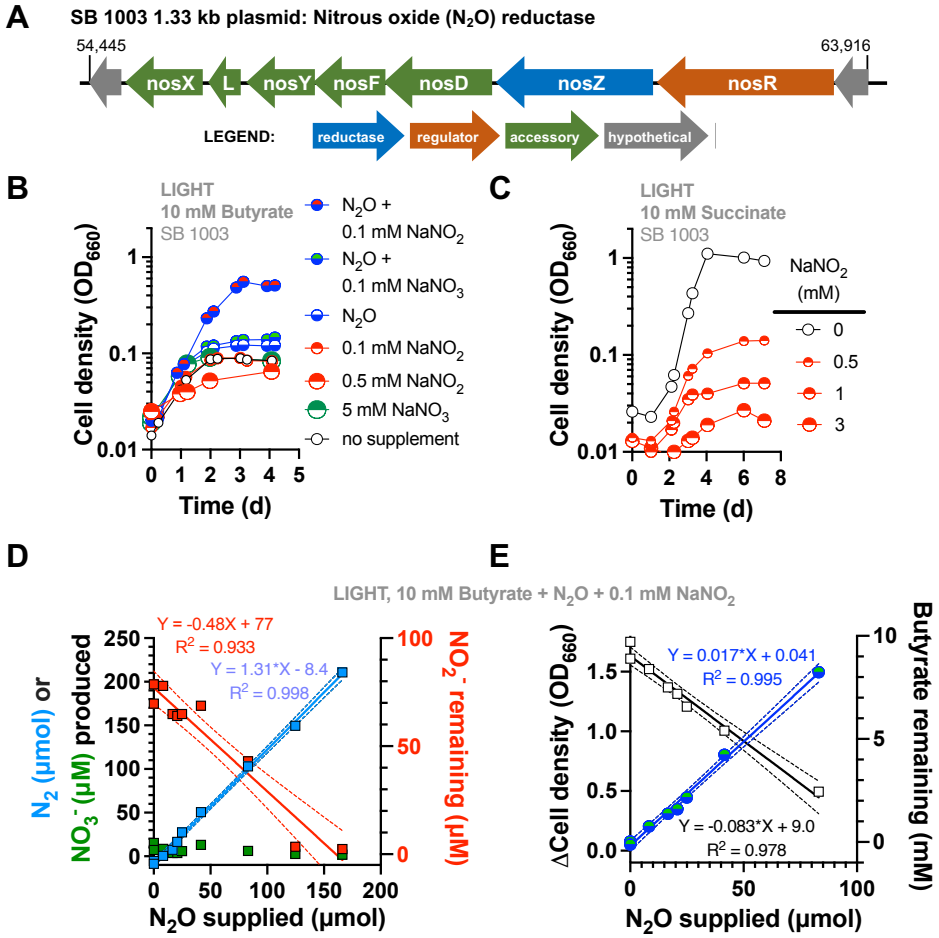

Fig. 8. $NaNO_2$ is required for photoheterotrophic N_2O reduction by *R. capsulatus* SB1003. **A.** Plasmid location of predicted N_2O reductase genes (*nos*). Numbers indicate nucleotide positions. **B.** Phototrophic growth with butyrate and various denitrification intermediates. Single representatives are shown. Similar trends observed for three biological replicates. Cultures had a 100% Ar headspace unless N_2O is indicated (100% N_2O). **C.** Phototrophic growth with succinate and various $NaNO_2$ concentrations to determine the toxicity limit. Single representatives were surveyed. **D, E.** Changes in N_2, NO_3^-, cell density, and butyrate in N_2O-limited cultures. Measurements were taken at inoculation and when the maximum cell density was reached. Each point represents a single independent culture. Samples were diluted in cuvettes where necessary to ensure linear correlation between OD and cell density. Most or all N_2O was removed by stationary phase. Linear regression for NO_2^- (**D**) gave a slope that was significantly different from zero (p-value = 0.0002).

again suggesting that the activity was not associated with a canonical denitrification reaction. Similar to *R. palustris*, the SB1003 chemotrophic growth rate and growth yield were lower than those in phototrophic conditions, and more electrons in butyrate were diverted to N_2O reduction compared to biosynthesis (Table 1). However, SB1003 appears to be capable of a 2.4-fold higher specific N_2O reduction rate, which is likely behind the proportionately higher chemotrophic growth rate compared to *R. palustris* CGA0092 (Table 1).

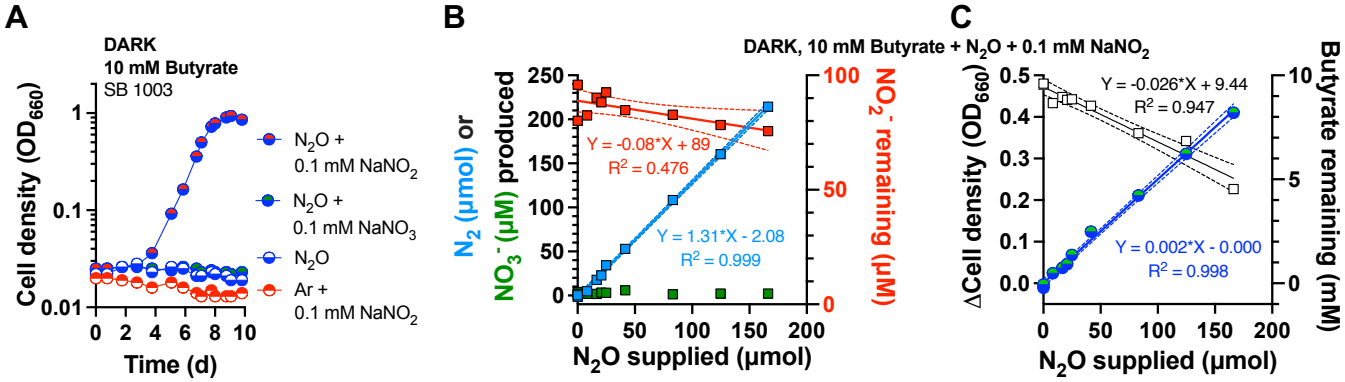

Fig. 9. $NaNO_2$ is required for N_2O respiration by SB1003 in the dark. A. Chemotrophic growth of SB1003 on butyrate with N_2O as an electron acceptor. Single representatives are shown. Similar trends were observed for three biological replicates. Cultures had a 100% Ar headspace unless N_2O is indicated (100% N_2O). **B, C.** Changes in N_2, NO_3^-, cell density, and butyrate in N_2O-limited cultures. Measurements were taken at inoculation and when the maximum cell density was reached. Each point represents a single independent culture. Most or all N_2O was removed by stationary phase. Linear regression for NO_2^- (**B**) gave a slope that was significantly different from zero (p-value = 0.0097).

Discussion

Here we verified that *R. palustris* CGA0092 and *R. capsulatus* SB1003 are partial denitrifiers, with each being capable of respiring the nitric oxides predicted from their genome annotations. We observed that these bacteria can only reduce N_2O when supplied with other denitrification intermediates. Most importantly, nitrogen oxides required for N_2O reduction include those outside of each organism's partial denitrification repertoire, that is, NO_3^- in the case of CGA0092 and NO_2^- in the case of SB1003.

NO_3^- as a non-catalyzable inducer of *nos* gene expression. Using a LacZ reporter under control of an *R. palustris nosR* promoter, we found that N_2O reduction is induced by NO_3^- and NO_2^-, at least in part, at the level of gene expression (our construct likely captures transcriptional and translational regulatory features). The level of induction was low compared to the 10-fold increase seen with a *B. diazoefficiens nosZ–lacZ* reporter (24, 33). One possible explanation for the discrepancy is our use of a *nosR* promoter–*lacZ* fusion. NosR is a required regulatory protein for nitrous oxide reductase activity (34, 35) that is typically encoded with little to no intergenic region between *nosR* and *nosZ* (Fig. 1). While the *nosR* promoter drives *nosZ* expression in some bacteria (23), in other bacteria *nosZ* expression can occur from separate, and sometimes multiple, transcriptional start sites (25, 36). Substantial work beyond the current study will be necessary to decipher the transcriptional and post-transcriptional regulatory mechanisms governing *R.*

palustris nos genes. However, our findings clearly indicate that NO_3^- or NO_2^- are required for N_2O reduction by *R. palustris* CGA0092, and that they play a role as inducers of *nos* gene expression.

Modification of NO_2^- and NO_3^-? A caveat to the observed activation of N_2O reduction activity by NO_2^- and NO_3^- is that some promiscuous biotic or abiotic transformation could be necessary to generate the inducing/activating molecule. We hypothesize that a promiscuous enzyme activity led to the slow NO_2^- removal in SB1003 cultures (Fig. 8, 9). One possible candidate is sulfite reductase (CysIJ; RCAP_rcc01594 and 03007), which bears homology to assimilatory nitrite reductase. In *E. coli*, CysIJ can convert NO_2^- to NH_4^+ 1.7-times faster than sulfite reduction but with a 200-fold lower affinity for NO_2^- compared to sulfite (k_m = 0.8 mM NO_2^-, 8-times above the concentration used in our SB1003 experiments) (37). If CysIJ was responsible for NO_2^- removal, then NO_2^- was likely the molecule activating N_2O reduction because CysIJ would convert NO_2^- to NH_4^+, which was already present at mM concentrations in the growth medium. However, there could be another enzymatic or spontaneous activity reducing NO_2^- to NO as a separate inducing molecule. For CGA0092, levels of N_2O reductase-inducing NO_3^- were stable. However, it is still possible that some of the 100 µM NO_3^- was converted below our detection limit to NO_2^- and/or NO. These molecules can induce N_2O reductase in other organisms like *P. aeruginosa*, although they are typically applied at µM or mM levels (23).

Possible regulators of N_2O reduction. Our work calls for future investigation into the regulatory mechanisms controlling N_2O reduction in CGA0092 and SB1003. However, we can speculate on the regulatory proteins involved based on genome annotations. In considering NO_3^- as an inducing molecule in CGA0092, NasTS stands out as a candidate. In *Bradyrhizobium diazoefficiens*, NasTS controls the transcriptional activation of *nos* genes (24, 25). CGA0092 has genes with significant sequence identity to *B. diazoefficiens* NasTS (77 and 66%, respectively; Fig. 1B). NnrR (Fig. 1B) could also be involved in regulating N_2O reductase, though more likely in response to NO (1, 23, 38-40).

NO_2^- could also activate N_2O reduction in SB1003 via an NnrR-like regulator. SB1003 has several CRP/Fnr-family transcriptional regulator genes encoded in its chromosome with >25% amino acid identity to denitrification regulators like *P. denitrificans* FnrP (RCAP_rcc02493; 74% identity) and *Pseudomonas aeruginosa* Dnr/NnrR (e.g., RCAP_rcc00107; 36% identity). One or more of these regulators could be involved in regulating N_2O reductase, though more likely in response to NO generated biotically or abiotically from NO_2^- (23).

Denitrification inventories should consider both reductases and regulators. Denitrification gene inventories are notoriously inconsistent with organismal phylogeny; it is common for one species to carry more or less denitrification genes than a close relative (8-10, 12, 41, 42). This inconsistency is also true for strains of *R. palustris* and *R. capsulatus* (20, 43-46). In some cases, horizontal gene transfer (HGT) could explain the phylogenetic discrepancies. The location of the *nos* operon on a plasmid in SB1003 is a straight-forward example of HGT (Fig. 8A). However, HGT cannot explain many of the chromosomal phylogenetic discrepancies. Phylogenetic analyses have suggested the involvement of other factors like gene duplication and divergence, lineage sorting (41), and gene loss (12). Gene loss could be advantageous in communities where there are redundant denitrification functions. As proposed in the Black Queen Hypothesis (47),

gene loss can occur when the cost of producing something outweighs the benefit of obtaining it from a neighbor. In this case, the cost of a full denitrification pathway could drive loss of denitrification genes if sufficient energy can be obtained by using a denitrification intermediate released by a neighbor (12). Benefits of partial denitrification pathways have been demonstrated using a synthetic community, though the benefits stemmed more from NO_2^- detoxification than energy savings (48).

Inventories of denitrification regulators have not received the same level of phylogenetic scrutiny as the reductases. Such analyses would be complicated by the fact that phylogenetically similar regulators can regulate different genes (49). However, regulator inventories are likely an important determinant of reductase inventories because improper regulation could influence maintenance or loss of a reductase gene. Regulator inventories also raise questions about the evolutionary histories of denitrification genes. For example, if NasTS is required for expression of the *nos* operon in *R. palustris* CGA0092, were both regulator and reductase genes serendipitously acquired at the same time as separate DNA molecules by HGT or were they acquired together as a single DNA molecule and then physically separated through genome rearrangements (Fig. 1B)? Alternatively, perhaps the common ancestor to CGA0092 and *B. diazoefficiens* USDA110 was capable of complete denitrification and CGA0092 lost nitrate reductase genes but retained the native regulatory network that was responsive to NO_3^-. Both genera clade together within the Nitrobacteraceae family but the CGA0092 genome is 3.4 Mb smaller than that of USDA110 and in each case the NasTS and the *nos* genes are separated by large stretches of chromosome (~ 2Mb in CGA0092 and ~5Mb in USDA110). Regulator inventory might also support a community role for partial denitrifiers. The regulation of N_2O reductase by NO_3^- and NO_2^- in this study could suggest that CGA0092 and SB1003 are primed to sense signals by denitrifying partners.

Our findings suggest that within communities of partial denitrifiers, nitric oxides are not only cross-fed metabolites but also important regulatory molecules. The requirement of these molecules for N_2O reduction is an important consideration in efforts to mitigate greenhouse gas emissions from agricultural soils, which is the largest source of N_2O emissions (6). Given that agricultural soils are fertilized with NO_3^-, we do not anticipate a shortage of NO_3^- in those environments. However, our findings expose a potential pitfall in overlooking the capacity of *nosZ*-harboring bacteria to reduce N_2O, if unanticipated inducing molecules are omitted from lab cultures.

Methods

Strains. *R. palustris* CGA0092 is a chloramphenicol-resistant type strain derived from CGA001 and differs from CGA009 by a single nucleotide polymorphism (13, 14). The Calvin cycle mutant Δ*cbbLSMP*::km^R (ΔCalvin, CGA4008) was constructed by deleting *cbbLS*, encoding ribulose-1,5-bisphosphate carboxylase (Rubisco) form I, in a previously described mutant lacking Rubisco form II (Δ*cbbM*; CGA668; (26)) via introduction of the suicide vector pJQΔ*cbbLS* (50) by conjugation with *E. coli* S17 as described (50, 51). The gene encoding phosphoribulokinase, *cbbP*, was then deleted in the resulting strain (Δ*cbbLSM*; CGA4006) by introducing the suicide vector pJQΔ*cbbP*::km^r (50), as above, to generate the Δ*cbbLSMP*::km^R strain, CGA4008. The elimination of three genes unique to the Calvin cycle greatly decreases the

odds of enriching for suppressor mutations. All strain genotypes were verified by PCR and Sanger sequencing. CGA4011 is a NifA* derivative of CGA4008 that has constitutive nitrogenase activity/H_2 production (50). *R. capsulatus* SB1003 was provided courtesy of Carl Bauer (Indiana University).

CGA4070 was derived from CGA0092 for assaying *nosR* promoter activity using a *lacZ* reporter chromosomally integrated upstream of the *nos* gene cluster, a similar strategy as that used in *B. diazoefficiens* (24, 52). Briefly, a 398-nt region upstream of the *nosR* start codon was synthesized in front of *lacZ* and incorporated into pTwist Kan High Copy plasmid by Twist Bioscience (twistdna.com) to create pTwist_PNos-LacZ. CGA0092 was transformed with pTwist_PNos-LacZ by electroporation and plated on photosynthetic medium (PM) agar with 10 mM succinate and 100 µg/ml kanamycin. Colonies were screened for integration by both PCR and by the appearance of blue color when patched to identical agar that also contained 5-bromo-4-chloro-3-indolyl-β-D-galactoside.

Growth conditions. Strains were routinely cultivated in 10 ml PM in 27-ml anaerobic test tubes. PM is based on described media compositions (53, 54) and contains (final concentrations): 12.5 mM Na_2HPO_4, 12.5 mM KH_2PO_4, 7.5 mM $(NH_4)_2SO_4$, 0.1 mM $Na_2S_2O_3$, 15 µM p-aminobenzoic acid, and 1 ml/L concentrated base (54). Concentrated base contains: 20 g/L nitriloacetic acid, 28.9 g/L $MgSO_4$, 6.67 g/L $CaCl_2 \cdot 2H_2O$, 0.019 g/L $(NH_4)_6Mo_7O_{24} \cdot 4H_2O$, 0.198 g/L $FeSO_4 \cdot 7H_2O$, and 100 ml/L Metals 44 (55). Metals 44 contains: 2.5 g/L ethylenediaminetetraacetic acid, 10.95 g/L $ZnSO_4 \cdot 7H_2O$, 5 g/L $FeSO_4 \cdot 7H_2O$, 1.54 g/L $MnSO_4 \cdot H_2O$, 0.392 g/L $CuSO_4 \cdot 5H_2O$, 0.25 g/L $Co(NO_3)_2 \cdot 6H_2O$, 0.177 g/L $Na_2B_4O_7 \cdot 10H_2O$. PM was made anaerobic by bubbling tubes with 100% Ar then sealing with rubber stoppers and aluminum crimps prior to autoclaving. After autoclaving, tubes were supplemented with either 20 mM sodium acetate, 10 mM sodium butyrate, or 10 mM disodium succinate from 100X anaerobic stock solutions. Where indicated, cultures were additionally supplemented with 20 mM $NaHCO_3$. SB1003 cultures were also supplemented with 0.1 µg/ml nicotinic acid, 0.2 µg/ml riboflavin, and 1.3 µg/ml thiamine-HCl. $NaNO_2$ or $NaNO_3$ were added from anaerobic stock solutions to the final concentrations indicated in the text. For conditions with N_2O, tubes were flushed with 100% N_2O through a 0.45 µm syringe filter and needle after all liquid supplements were added. A second needle was used for off-gassing. For N_2O-limited cultures, the indicated volume of filtered gas was added via syringe. Cultures were inoculated with a 1% inoculum from starter cultures grown phototrophically in anaerobic PM with succinate, except for the experiment testing Calvin cycle mutants (Fig. 3C) in which all starter cultures were grown aerobically in 3 ml PM with succinate in the dark. These aerobic conditions were used to accommodate the Δ*cbbLSMP*::km^R mutant (CGA4008) that requires an electron sink to grow.

Analytical procedures. Culture growth was monitored via optical density at 660 nm (OD_{660}) using a Genesys 20 spectrophotometer (Thermo-Fisher, Waltham, MA, USA) directly in culture tubes without sampling. For N_2O-limitted cultures, samples were diluted in cuvettes where specified. Specific growth rates were calculated using OD_{660} values between 0.1 and 1.0 where cell density and OD are linearly correlated. N_2, N_2O, and H_2 were sampled from culture headspace using a gas-tight syringe and analyzed using a Shimadzu GC-2014 gas chromatograph (GC) equipped with a thermal conductivity detector. GC conditions for H_2 were described previously (56). GC conditions for N_2 and N_2O used He as a carrier gas at 20 ml/min, a

80/100 Porapak N column (6' x 1/8" x 2.1 mm; Supelco) at 170 ºC, an inlet temperature of 120ºC, and a detector temperature of 155ºC with a current of 150 mA. Gas standards were prepared by injecting specific volumes of 1 ATM of pure gasses (41.6 mM based on the ideal gas law and a temperature of 293 K) into a stopper-sealed serum vial of known volume, containing with a few glass beads to aid in mixing. Gas standards were mixed by shaking, sampled with a gas-tight syringe, and then injected at 1 ATM by releasing pressure prior to injection. Pressure was not released prior to injection for culture headspace samples. Syringes were flushed with He prior to each standard and culture injection to minimize contamination with atmospheric N_2. NO_3^- and NO_2^- were measured using a colorimetric Griess assay kit according to the manufacturer's instructions (Cayman Chemical). Conversion of NO_3^- to NO_2^- was accomplished via NO_3^- reductase provided with the kit. N_2, N_2O, NO_3^- and NO_2^- were measured at the time of inoculation and at stationary phase.

β-galactosidase reporter assays. *R. palustris* strains were grown to mid-late exponential phase (0.4 - 1.1 OD_{660}) with 23 mM sodium acetate and either 0.1 mM NaCl, $NaNO_3$, or $NaNO_2$, with or without 4 ml N_2O. Cultures were then chilled on ice and all subsequent processing was carried out between 0 - 4 ºC. Cells were harvested by centrifugation, supernatants were discarded, and cells were resuspended in 0.5 ml Z-buffer. Cells were lysed by five 20-s rounds of bead beating at maximum speed using a FastPrep®-24 benchtop homogenizer (MP Biomedical), with 5 min on ice between rounds. Cell debris was pelleted by centrifugation and supernatant protein was quantified using Bio-Rad's Bradford assay kit. Cell lysate (50 µl supernatant) was mixed with 100 µl Z-buffer in wells of a 96-well plate. Reactions were started with the addition of 30 µl of 4 mg/ml ortho-nitrophenyl-ß-galactoside. Formation of *o*-nitrophenol was monitored at 420 nm over time at 30ºC using a BioTek Synergy plate reader. Specific activity was determined by linear regression of the initial velocity and normalized for protein concentration.

Bioinformatics. PSI-BLAST used default parameters except for 500 targets, an expect threshold of 10, a word size of 3, and a PSI-BLAST threshold of 0.005 using the refseq_protein database for bacteria. At least five iterations were run or until no further sequences were found. Accession numbers for the query sequences are in Table S1.

Statistical analyses. Graphpad Prism v10 was used for all statistical analyses.

Acknowledgements

This work was supported in part by a National Science Foundation CAREER award (MCB-1749489NSF), the Division of Chemical Sciences, Geosciences, and Biosciences, Office of Basic Energy Sciences, U.S. Department of Energy (DOE), through Grant DE-FG02-05ER15707, the Office of Science (BER), U.S. Department of Energy, through Grant DE-FG02-07ER64482, and the Indiana University College of Arts and Sciences. We are grateful to Doug Rusch, Julia van Kessel, Cristina Landeta, Nick Haas, José Heerdink-Santos, Jillian Lewis, William Rockliff, and Anika Hays for advice, reagents, and media preparation. We are also grateful to the anonymous reviewers for constructive feedback.

References

1. Zumft WG. 1997. Cell biology and molecular basis of denitrification. Microbiol Mol Biol Rev 61:533-616.
2. Zumft WG, Kroneck PM. 2007. Respiratory transformation of nitrous oxide (N_2O) to dinitrogen by Bacteria and Archaea. Adv Microb Physiol 52:107-227.
3. Lundberg JO, Weitzberg E, Cole JA, Benjamin N. 2004. Nitrate, bacteria and human health. Nat Rev Microbiol 2:593-602.
4. Portmann RW, Daniel JS, Ravishankara AR. 2012. Stratospheric ozone depletion due to nitrous oxide: influences of other gases. Philos Trans R Soc Lond B Biol Sci 367:1256-64.
5. Barnard R, Leadly P, Hungate B. 2005. Global change, nitrification, and denitrification: A review. Global Biogeochem Cycles 19:327-338.
6. Reay DS, Davidson EA, Smith KA, Smith P, Melillo JM, Dentener F, Crutzen PJ. 2012. Global agriculture and nitrous oxide emissions. Nat Clim Change 2:410-416.
7. Roco CA, Bergaust LL, Bakken LR, Yavitt JB, Shapleigh JP. 2017. Modularity of nitrogen-oxide reducing soil bacteria: linking phenotype to genotype. Environ Microbiol 19:2507-2519.
8. Lycus P, Lovise Bothun K, Bergaust L, Peele Shapleigh J, Reier Bakken L, Frostegard A. 2017. Phenotypic and genotypic richness of denitrifiers revealed by a novel isolation strategy. ISME J 11:2219-2232.
9. Gowda K, Ping D, Mani M, Kuehn S. 2022. Genomic structure predicts metabolite dynamics in microbial communities. Cell 185:530-546 e25.
10. Graf DR, Jones CM, Hallin S. 2014. Intergenomic comparisons highlight modularity of the denitrification pathway and underpin the importance of community structure for N2O emissions. PLoS One 9:e114118.
11. Zhang IH, Sun X, Jayakumar A, Fortin SG, Ward BB, Babbin AR. 2023. Partitioning of the denitrification pathway and other nitrite metabolisms within global oxygen deficient zones. ISME Commun 3:76.
12. Hallin S, Philippot L, Loffler FE, Sanford RA, Jones CM. 2018. Genomics and Ecology of Novel N_2O-Reducing Microorganisms. Trends Microbiol 26:43-55.
13. Larimer FW, Chain P, Hauser L, Lamerdin J, Malfatti S, Do L, Land ML, Pelletier DA, Beatty JT, Lang AS, Tabita FR, Gibson JL, Hanson TE, Bobst C, Torres JLTy, Peres C, Harrison FH, Gibson J, Harwood CS. 2004. Complete genome sequence of the metabolically versatile photosynthetic bacterium *Rhodopseudomonas palustris*. Nat Biotechnol 22:55-61.
14. Mazny BE, Sheff OF, LaSarre B, McKinlay A, McKinlay JB. 2023. Complete genome sequence of *Rhodopseudomonas palustris* CGA0092 and corrections to the *R. palustris* CGA009 genome sequence. Microbiol Resour Announc 12:e0128522.
15. Luxem KE, Kraepiel AML, Zhang L, Waldbauer JR, Zhang X. 2022. Corrigendum. Carbon substrate re-orders relative growth of a bacterium using Mo-, V-, or Fe-nitrogenase for nitrogen fixation. Environ Microbiol 24:2170-2176.
16. Luxem KE, Kraepiel AML, Zhang L, Waldbauer JR, Zhang X. 2020. Carbon substrate re-orders relative growth of a bacterium using Mo-, V-, or Fe-nitrogenase for nitrogen fixation. Environ Microbiol 22:1397-1408.

17. Oda Y, Larimer FW, Chain PSG, Malfatti S, Shin MV, Vergez LM, Hauser L, Land ML, Braatsch S, Beatty JT, Pelletier DA, Schaefer AL, Harwood CS. 2008. Multiple genome sequences reveal adaptations of a phototrophic bacterium to sediment microenvironments. Proc Natl Acad Sci USA 105:18543-18548.
18. Altschul SF, Madden TL, Schaffer AA, Zhang J, Zhang Z, Miller W, Lipman DJ. 1997. Gapped BLAST and PSI-BLAST: a new generation of protein database search programs. Nucleic Acids Res 25:3389-402.
19. McKinlay JB, Harwood CS. 2011. Calvin cycle flux, pathway constraints, and substrate oxidation state together determine the H_2 biofuel yield in photoheterotrophic bacteria. mBio 2:e00323-10.
20. Richardson DJ, King GF, Kelly DJ, McEwan AG, Ferguson SJ, Jackson JB. 1998. The role of auxiliary oxidants in maintaining redox balance during phototrophic growth of *Rhodobacter capsulatus* on propionate or butyrate. Arch Microbiol 150:131-7.
21. Härtig E, Zumft WG. 1999. Kinetics of *nirS* expression (cytochrome cd1 nitrite reductase) in *Pseudomonas stutzeri* during the transition from aerobic respiration to denitrification: evidence for a denitrification-specific nitrate- and nitrite-responsive regulatory system. J Bacteriol 181:161-6.
22. Sabaty M, Schwintner C, Cahors S, Richaud P, Vermeglio A. 1999. Nitrite and nitrous oxide reductase regulation by nitrogen oxides in *Rhodobacter sphaeroides* f. sp. denitrificans IL106. J Bacteriol 181:6028-32.
23. Arai H, Mizutani M, Igarashi Y. 2003. Transcriptional regulation of the nos genes for nitrous oxide reductase in *Pseudomonas aeruginosa*. Microbiol 149:29-36.
24. Sanchez C, Itakura M, Okubo T, Matsumoto T, Yoshikawa H, Gotoh A, Hidaka M, Uchida T, Minamisawa K. 2014. The nitrate-sensing NasST system regulates nitrous oxide reductase and periplasmic nitrate reductase in *Bradyrhizobium japonicum*. Environ Microbiol 16:3263-74.
25. Sanchez C, Mitsui H, Minamisawa K. 2017. Regulation of nitrous oxide reductase genes by NasT-mediated transcription antitermination in *Bradyrhizobium diazoefficiens*. Environ Microbiol Rep 9:389-396.
26. McKinlay JB, Harwood CS. 2010. Carbon dioxide fixation as a central redox cofactor recycling mechanism in bacteria. Proc Natl Acad Sci USA 107:11669-11675.
27. McCully AL, Onyeziri MC, LaSarre B, Gliessman JR, McKinlay JB. 2020. Reductive tricarboxylic acid cycle enzymes and reductive amino acid synthesis pathways contribute to electron balance in a *Rhodospirillum rubrum* Calvin-cycle mutant. Microbiol 166:199-211.
28. Falcone DL, Tabita FR. 1991. Expression of endogenous and foreign ribulose 1,5-bisphosphate carboxylase-oxygenase (RubisCO) genes in a RubisCO deletion mutant of *Rhodobacter sphaeroides*. J Bacteriol 173:2099-108.
29. Hallenbeck PL, Lerchen R, Hessler P, Kaplan S. 1990. Roles of CfxA, CfxB, and external electron acceptors in regulation of ribulose 1,5-bisphosphate carboxylase/oxygenase expression in *Rhodobacter sphaeroides*. J Bacteriol 172:1736-48.
30. Sauer U, Lasko DR, Fiaux J, Hochuli M, Glaser R, Szyperski T, Wuthrich K, Bailey JE. 1999. Metabolic flux ratio analysis of genetic and environmental modulations of *Escherichia coli* central carbon metabolism. J Bacteriol 181:6679-88.

31. McKinlay JB, Shachar-Hill Y, Zeikus JG, Vieille C. 2007. Determining *Actinobacillus succinogenes* metabolic pathways and fluxes by NMR and GC-MS analyses of ^{13}C-labeled metabolic product isotopomers. Metab Eng 9:177-92.
32. McCully AL, LaSarre B, McKinlay JB. 2017. Growth-independent cross-feeding modifies boundaries for coexistence in a bacterial mutualism. Environ Microbiol 19:3538-3550.
33. Sanchez C, Itakura M, Mitsui H, Minamisawa K. 2013. Linked expressions of nap and nos genes in a *Bradyrhizobium japonicum* mutant with increased N_2O reductase activity. Appl Environ Microbiol 79:4178-80.
34. Cuypers H, Viebrock-Sambale A, Zumft WG. 1992. NosR, a membrane-bound regulatory component necessary for expression of nitrous oxide reductase in denitrifying *Pseudomonas stutzeri*. J Bacteriol 174:5332-9.
35. Velasco L, Mesa S, Xu CA, Delgado MJ, Bedmar EJ. 2004. Molecular characterization of *nosRZDFYLX* genes coding for denitrifying nitrous oxide reductase of *Bradyrhizobium japonicum*. Antonie Van Leeuwenhoek 85:229-35.
36. Cuypers H, Berghofer J, Zumft WG. 1995. Multiple *nosZ* promoters and anaerobic expression of nos genes necessary for *Pseudomonas stutzeri* nitrous oxide reductase and assembly of its copper centers. Biochim Biophys Acta 1264:183-90.
37. Siegel LM, Davis PS, Kamin H. 1974. Reduced nicotinamide adenine dinucleotide phosphate-sulfite reductase of enterobacteria. 3. The *Escherichia coli* hemoflavoprotein: catalytic parameters and the sequence of electron flow. J Biol Chem 249:1572-86.
38. Gaimster H, Alston M, Richardson DJ, Gates AJ, G R. 2018. Transcriptional and environmental control of bacterial denitrification and N_2O emissions. FEMS Micobiol Lett 365:fnx277.
39. Bergaust L, van Spanning RJM, Frostegard A, Bakken LR. 2012. Expression of nitrous oxide reductase in *Paracoccus denitrificans* is regulated by oxygen and nitric oxide through FnrP and NNR. Microbiol 158:826-834.
40. Torres MJ, Simon J, Rowley G, Bedmar EJ, Richardson DJ, Gates AJ, Delgado MJ. 2016. Nitrous oxide metabolism in nitrate-reducing bacteria: physiology and regulatory mechanisms. Adv Microb Physiol 68:353-432.
41. Jones CM, Stres B, Rosenquist M, Hallin S. 2008. Phylogenetic analysis of nitrite, nitric oxide, and nitrous oxide respiratory enzymes reveal a complex evolutionary history for denitrification. Mol Biol Evol 25:1955-66.
42. Barth KR, Isabella VM, Clark VL. 2009. Biochemical and genomic analysis of the denitrification pathway within the genus *Neisseria*. Microbiol 155:4093-4103.
43. Klemme J-H, Chyla I, Preuss M. 1980. Dissimilatory nitrate reduction by strains of the facultative phototrophic bacterium *Rhodopseudomonas palustris*. FEMS Microbiol Lett 9:137-140.
44. McEwan AG, Greenfield AJ, Wetzstein HG, Jackson JB, Ferguson SJ. 1985. Nitrous oxide reduction by members of the family *Rhodospirillaceae* and the nitrous oxide reductase of *Rhodopseudomonas capsulata*. J Bacteriol 164:823-30.
45. Rayyan A, Meyer T, Kyndt J. 2018. Draft whole-genome sequence of the purple photosynthetic bacterium *Rhodopseudomonas palustris* XCP. Microbiol Resour Announc 7:e00855-18.

599 46. Richardson DJ, Bell LC, Moir JWB, Ferguson SJ. 1994. A denitrifying strain of *Rhodobacter*
600 *capsulatus*. FEMS Micobiol Lett 120:323-8.
601 47. Morris JJ, Lenski RE, Zinser ER. 2012. The Black Queen Hypothesis: Evolution of
602 dependencies through adaptive gene loss. mBio 3:e00036-12.
603 48. Lilja EE, Johnson DR. 2016. Segregating metabolic processes into different microbial cells
604 accelerates the consumption of inhibitory substrates. ISME J 10:1568-1578.
605 49. Perez JC, Groisman EA. 2009. Evolution of transcriptional regulatory circuits in bacteria.
606 Cell 138:233-44.
607 50. Gordon GC, McKinlay JB. 2014. Calvin cycle mutants of photoheterotrophic purple
608 nonsulfur bacteria fail to grow due to an electron imbalance rather than toxic
609 metabolite accumulation. J Bacteriol 196:1231-7.
610 51. Rey FE, Oda Y, Harwood CS. 2006. Regulation of uptake hydrogenase and effects of
611 hydrogen utilization on gene expression in *Rhodopseudomonas palustris*. J Bacteriol
612 188:6143-6152.
613 52. Mesa S, Bedmar EJ, Chanfon A, Hennecke H, Fischer HM. 2003. *Bradyrhizobium*
614 *japonicum* NnrR, a denitrification regulator, expands the FixLJ-FixK2 regulatory cascade.
615 J Bacteriol 185:3978-82.
616 53. Kim M-K, Harwood CS. 1991. Regulation of benzoate-CoA ligase in *Rhodopseudomonas*
617 *palustris*. FEMS Microbiol Lett 83:199-203.
618 54. Ornston LN, Stanier RY. 1966. The conversion of catechol and protocatechuate to beta-
619 ketoadipate by *Pseudomonas putida*. J Biol Chem 241:3776-86.
620 55. Cohen-Bazire G, Sistrom WR, Stanier RY. 1957. Kinetic studies of pigment synthesis by
621 non-sulfur purple bacteria. J Cell Comp Physiol 49:25-68.
622 56. Huang JJ, Heiniger EK, McKinlay JB, Harwood CS. 2010. Production of hydrogen gas from
623 light and the inorganic electron donor thiosulfate by *Rhodopseudomonas palustris*. Appl
624 Environ Microbiol 76:7717-7722.
625